Research Article

Entao Shi, Yongmei Wang*, Nan Jia, Jinghua Mao, Guanda Lu and Shaolin Liang

Absorbing Aerosol Sensor on Gao-Fen 5B satellite

https://doi.org/10.1515/aot-2018-0040
Received August 14, 2018; accepted October 23, 2018

Abstract: The Absorbing Aerosol Sensor (AAS) will be launched aboard the GaoFen-5B satellite in China. The main purpose of AAS is to monitor absorbing aerosols by measuring the solar backscatter radiation. AAS is an ultraviolet-visible imaging spectrometer that uses a single charge coupled device to capture both the spectrum and the cross-track direction with a 114° wide swath. The large field of view enables daily global coverage with 4-km spatial resolution. The spectral range of the instrument extends from 340 to 550 nm with spectral resolution (full width at half maximum) of 2 nm. This paper provides details of the instrument design, including system design, optical design, and mechanical design, as well as detector and calibration unit on orbit. The numerous simulations show that all design results satisfy the specification and vibration requirements of the instrument.

Keywords: absorbing aerosol; absorbing aerosol index; astigmatic telescope; imaging spectrometer; solar backscatter radiation.

***Corresponding author: Yongmei Wang,** Laboratory of Space Environment Exploration, National Space Science Center, Chinese Academy of Sciences, Beijing 100190, China; School of Astronomy and Space Science, University of Chinese Academy of Sciences, Beijing 100049, China; Beijing Key Laboratory of Space Environment Exploration, Beijing 100190, China; and Key Laboratory of Environmental Space Situation Awareness Technology, Beijing 100190, China, Tel.: +86-10-62582751, e-mail: wym@nssc.ac.cn
Entao Shi and Shaolin Liang: Laboratory of Space Environment Exploration, National Space Science Center, Chinese Academy of Sciences, Beijing 100190, China; School of Astronomy and Space Science, University of Chinese Academy of Sciences, Beijing 100049, China; Beijing Key Laboratory of Space Environment Exploration, Beijing 100190, China; and Key Laboratory of Environmental Space Situation Awareness Technology, Beijing 100190, China. http://orcid.org/0000-0001-6821-3318 (E. Shi)
Nan Jia, Jinghua Mao and Guanda Lu: Laboratory of Space Environment Exploration, National Space Science Center, Chinese Academy of Sciences, Beijing 100190, China

www.degruyter.com/aot

1 Introduction

Aerosol is an important but complicated factor in climate and atmospheric chemistry. Absorbing aerosol is a kind of aerosol, such as dust, biomass burning, and volcano ash. The absorbing aerosol index (AAI) indicates the presence of elevated levels of absorbing aerosols in the troposphere. It separates the spectral contrast at two ultraviolet (UV) wavelengths caused by absorbing aerosols from that of other effects, including molecular Rayleigh scattering, surface reflection, gaseous absorption, and aerosol and cloud scattering [1]. Because the surface albedos of land and ocean are smaller in the UV region than in the visible and near-infrared regions, this UV radiance should be suitable for aerosol detection over land.

A series of instruments, including TMOS (Total Map Ozone Suit) on NIMBUS-7 [2], GOME (Global Ozone Monitoring Instrument) on ERS-2, SCIAMACHY (Scanning Imaging Absorption Spectrometer for Atmospheric CartograpHY) on ENVISAT [3], OMI (Ozone Monitoring Instrument) on the EOS-AURA satellite [4], OMPS (Ozone Mapping Profiler Suite) on NPP/NPOESS [5], and TROPOMI on Sentinel-5P [6], have been used for ozone observation and aerosol retrieval products, which include the total of ozone and other trace gases, AAI, UV-aerosol optical depth, etc. [7, 8]. Moreover, TOU (Total Ozone Unit) on FY-3 [9] in China has also a total of ozone and AAI product with lower resolution. These products have been used for the global observation of ozone, heavy dust, biomass burning, volcanic eruption events, etc.

AAS is a UV-visible spectrograph that combines high spatial resolution and lower spectral resolution together with daily global coverage. The small ground pixel projection and high temporal resolution will contribute to the analysis of the source of air pollution. AAS is intended to serve as the first instrument for absorbing aerosol monitoring by measuring a continuous spectrum in the range of 340–550 nm in China. In this paper, we discuss the overall design of AAS.

2 System description

AAS is a wide field-of-view (FOV), pushbroom imaging spectrograph using a two-dimensional detector to achieve

Table 1: Specifications of AAS.

Index	Characteristics
Spectral range (nm)	340–550 nm
Spectral resolution (nm)	~2 nm
Field of view	±57°
Spatial resolution	4 km × 4 km (at nadir)
SNR	>1000 (10.89 μW/cm² · sr · nm)
Wavelength calibration accuracy	0.1 nm
Dynamic range	10^3
Stray light	10^{-3}

spectral and spatial imaging. One direction on the charge coupled device (CCD) corresponds to the large FOV across track to the flight direction; on another direction on the CCD, the spectrum is registered. Table 1 summarizes a number of important specifications of AAS.

AAS includes two major subassemblies: one is the optical bench, which is the heart of the instrument, and the other one is the electrical control unit. The optical bench consists of the telescope, spectrometer, detector module, and calibration unit. A polarization scrambler is placed in the optical path of the telescope to make the measurement insensitive to the polarization status of the incoming radiance.

Figure 1 shows the block diagram of the working principle of AAS. Atmospheric backscattered radiation entering the instrument is reflected by the primary mirror of the super-wide-angle telescope system, and is depolarized by the polarization scrambler, and then the incoming radiation is concentrated on the slit of the spectrometer by the second mirror of the telescope system. The light is collimated, dispersed, and then imaged onto the detector. The spectral and spatial distributions of the instantaneous FOV (IFOV) are detected by a two-dimensional CCD. Global coverage monitoring of aerosol is achieved by the IFOV detector and satellite motion.

To satisfy long-term stability operation over an 8-year lifetime, calibration on orbit, including irradiance and wavelength calibration, plays an important role. Two diffusers are used to measure solar irradiance. Wavelength calibration is performed by detection of the solar Fraunhofer lines during the solar calibration. Moreover, a preset white-light source (WLS) is used to monitor detector performance in-flight.

In order to ensure the stability of the instrument, a cooling system is needed. In this instrument, a thermal radiator is mounted to create a stable environment for detectors and optical bench. The operation temperature of the optical bench is 293 ± 2 K, and the detector will operate at <278 K.

The optical system, detector, calibration unit, and mechanism are described in detail in the following sections.

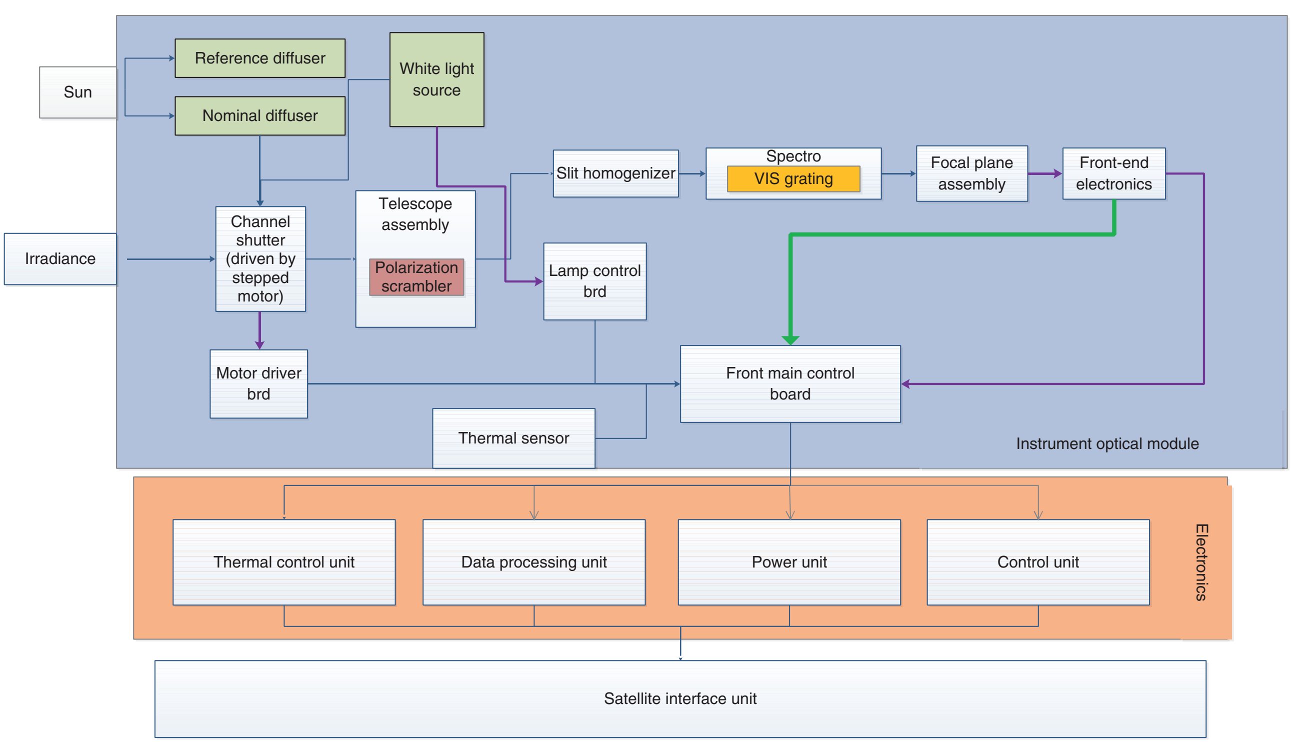

Figure 1: Functional schematic of AAS.

3 Descriptions of AAS

3.1 Telescope

The telescope of AAS images the back-scattering light of the atmosphere onto the spectrometer's entrance slit. The telescope has a very large FOV on cross-orbit direction or swath and a small FOV along the tracking direction in order to meet the requirements of global coverage and high spatial resolution. Some of the key parameters of the telescope are given in Table 2.

The AAS telescope is an anamorphic, astigmatic, reflective, two-concave-mirror, along tracking telecentric [10–12], cross-direction f-theta telescope. Anamorphic means the telescope has different powers at swath direction and along tracking direction, whereas astigmatic means the telescope has different back focal lengths at two directions. The two concave mirrors are referred to as primary mirror and secondary mirror, in the order of light from the atmosphere backscattered to the telescope. The two mirrors of the telescope have freeform surface compared with a spherical surface to meet the stringent spatial requirement; cross-direction f-θ means the image height is linear to the field angle at swath direction. The entrance pupil is imaged to infinity, which is equivalent to image telecentricity. The surface sag of the freeform mirrors [13] is illustrated in the following equation (Zemax user's manual):

$$Z=\frac{cr^2}{1+\sqrt{1-(1+k)c^2r^2}}+\sum_{i=1}^{N}A_iE_i(x,y) \tag{1}$$

The anamorphic telescope has two different F-numbers in the two perpendicular directions; this difference has been achieved by using a rectangle stop. The telescope further has different powers in the along tracking and swath directions, which are achieved using the different radii on freeform mirrors in two different directions. The optical system of the telescope is shown in Figure 2.

Table 2: Characteristics of the telescope.

Item	Unit	Value
Focal length (spectral)	mm	68
Focal length (spatial)	mm	34
Spectral range	nm	340–550
FOV	deg	114×0.18°
F/# (spectral)	–	F/9
F/# (spatial)	–	F/8
Telecentric	–	Yes
f-θ	–	Yes
Total length	mm	≤230

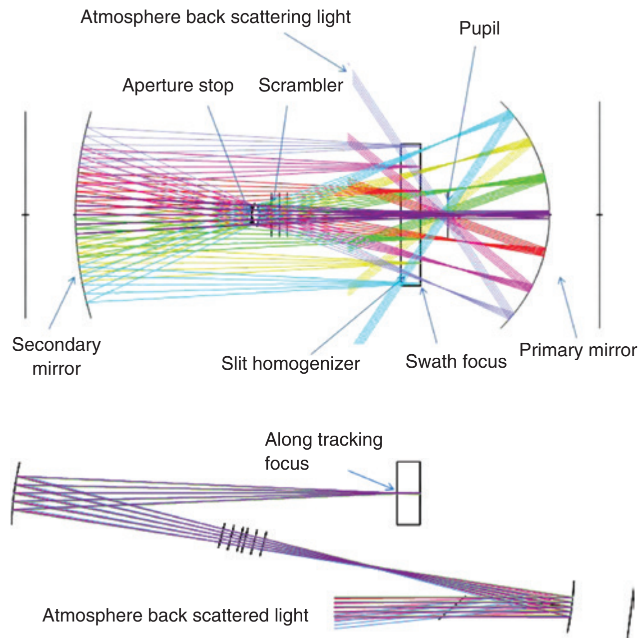

Figure 2: Telescope layout.

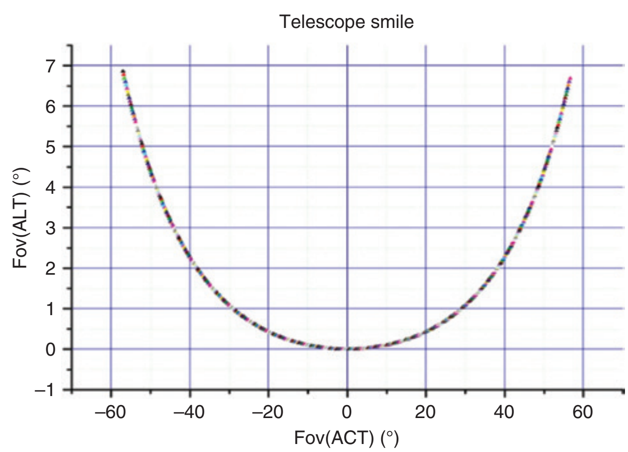

Figure 3: Ground projection of FOV.

The off-axis two freeform mirrors are adopted in the telescope system, and the tilt angle of each mirror and the optical axis is 6.5° to avoid obscuration. This off-axis structure of the mirror inevitably leads to off-axis distortion, which causes image bending. Deviations of FOV along the spectral direction ensure that the telescope image is straight. Thus, that a slit homogenizer could be used to mitigate the instrument spectral response function error. After optimization, the maximum FOV deviation is 6.8° at the edge of FOV. Due to the curvature of FOV, the shape of the FOV footprint projected on the ground in different FOVs changes from the rectangular shape of the conventional spectrometer to a diamond shape, as shown in Figure 3.

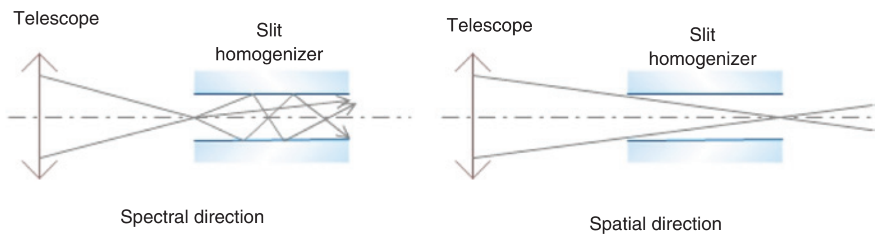

Figure 4: Schematic of slit.

3.2 Slit homogenizer

A slit homogenizer is used to mitigate the error of the exact shape of the lines in the measured spectrum [14]. The telescope is an astigmatism. At swath, the telescope and spectrometer are coupled to keep the spatial image resolution, while at the along tracking (ALT) direction, the telescope is focused at the slit homogenizer entrance. The scheme of the slit homogenizer is shown in Figure 4; the slit width is 0.24 mm, the length is 70 mm, and the slit thickness is 9.6 mm.

3.3 The spectrometer

The spectrometer includes a collimator system, a diffraction grating, and an imaging optical system. Figure 5 indicates the spectrometer optics for AAS from the telescope to image plane as modeled in Zemax. The view shown is the three-dimensional layout, and the rays are colored by wavelength. The collimator system adopts a refractive-reflective system [15]. After two stages of collimating, the parallelism of the outgoing beam is <5′. Then, the collimated beam is dispersed by a plane diffraction grating. Finally, the spectrum is imaged onto the detector by a camera lens. The collimated beam incidents to diffraction grating and dispersed to the imager, consisting two fused silica lenses and five CaF2 lenses, which focus different wavelengths of light to the detector. The parameters of the spectrum are listed in Table 3.

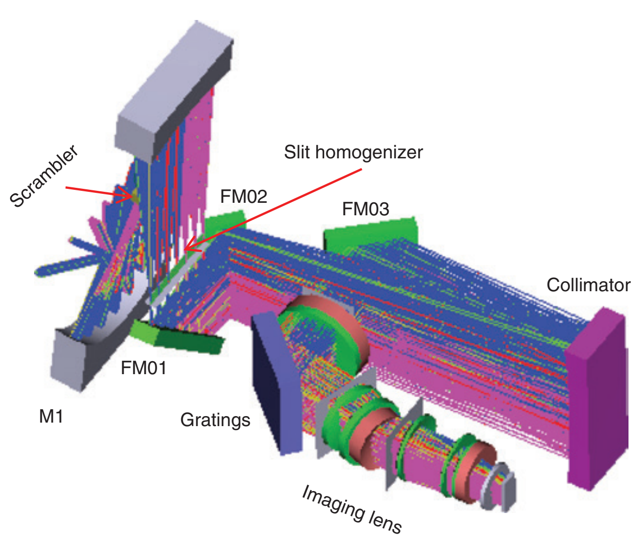

Figure 5: Optical schematic of AAS.

3.4 Detector

The AAS spectrometer will achieve a Signal-to-Noise Ratio (SNR) of >1000:1 in all spectral bands. A CCD from Teledyne E2V (UK) is used as detector. This CCD (55–30) device is split into an imaging section and a storage section, and each section has 1252(H) × 576(V) pixels with pixel size of 22.5 μm^2. The device utilizes the advanced inverted-mode operation to lower dark current and has high quantum efficiency at UV wavelength (UV enhanced). The device will be operated in a frame transfer mode. CCD preamplifier electronics are mounted closely to the associated focal plane assembly module (ASM) in optical assembly for minimizing the signal disturbance.

The optical bench is kept at room temperature (293 ± 2 K). However, the CCD module needs to be cooled in order to suppress the detector dark current. The CCD detector is operated at 278 ± 1 K. The temperature stability for both the optical module and the detector is at a high level in order to maintain the required radiometric accuracy.

3.5 Calibration unit

For ensuring the long-term stability requirement of 2% change over 8 years on orbit, the calibration unit is an important module. The calibration wheel includes solar irradiance measurement and internal calibration, which is driven by motor. For solar irradiance calibration, the calibration stability is maintained by periodic solar irradiance observation using two scatter diffusers. Calibration

Table 3: Spectrum parameters.

Parameter	Description	Unit	Value 1	Value 2
Wavelength range	Shortest/longest	nm	340 nm	550 nm
Spectral resolution	–	nm	2 nm	
Grating angle of incidence	–	deg	43.15°	
Grating diffraction order	–	–	1	
Grating line density	–	g/mm	300 g/mm	
Oversampling × pixel size	Spectral/spatial	µm	[4 × 2]:22.5 µm	
F/#	Spectral/spatial	–	F/9	F/8
Slit	Width/length	mm	0.24	70
Collimator focal length	Spectral/spatial	mm	376.5 mm	
Imager focal length	–	mm	86.28 mm	
Image height	Spectral/spatial	mm	10.19 mm/16.1 mm	

of the working diffuser is performed weekly and that of the reference diffuser once every 3 months, so as to minimize the influence of contamination. The light path for solar irradiance measurements is the same as the light path for Earth radiance measurements. In order to monitor the wavelength shift on orbit, wavelength calibration is performed during the solar calibration and atmospheric radiation measurement by using the spectral structure of the solar Fraunhofer lines [16].

Internal calibration is performed using WLS to monitor the non-uniformity response (pixel-to-pixel response non-uniformity) and the bad pixels of the detector. The WLS is a quartz foam halogen lamp (5 W and 12 V) that has good stability and repeatability. In the optical bench, the WLS illuminates the diffuser and is scattered to the telescope from the entrance pupil.

3.6 Mechanical design

The mechanical design of AAS adopted the modular construction concept. The mechanical module of AAS optical

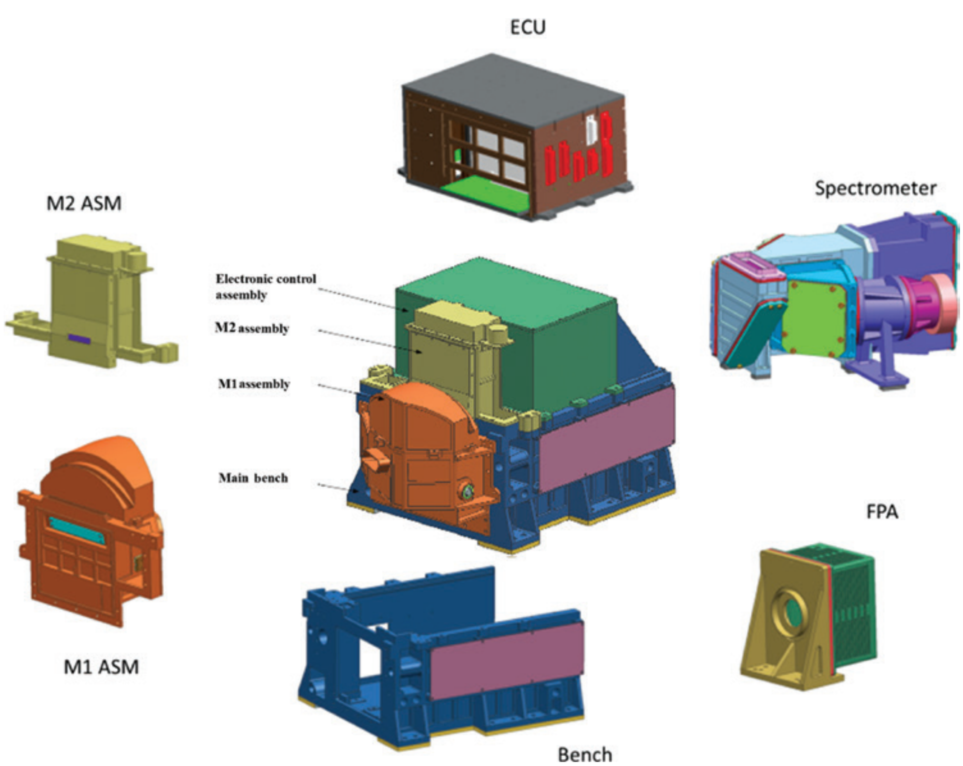

Figure 6: Mechanics of AAS.

subassembly includes M1 ASM, M2 ASM, optical bench, spectrometer module, focal plane ASM, and electronic control unit. This construction could ensure meeting the high-precision requirements of optical system tolerance, and easy mounting and alignment. The spectrometer module was insulated by titanic and polyimide spacer for the thermal stability requirement. The mechanics of AAS is shown in Figure 6.

A large number of numerical simulations have been performed to verify and support the mechanical design. This comprises finite element model, thermal analysis, and stiffness and strength calculations. In particular, a large effort was made to reduce the stresses exerted on the elements of the spectrometer optics. As a result, the spectrometer measurement would be affected in an unpredictable manner and after the calibration of the instrument. The simulation showed that the mechanical design can survive the launch vibrations and can also work stably in the space environment.

4 Conclusion

The AAS instrument will be launched aboard the Gao-Fen 5B satellite in 2020. AAS is a no-scanning nadir wide FOV imaging spectrometer that uses a two-dimensional detector to combine high spatial resolution and lower spectral resolution together with daily global coverage. All design results satisfy the specification requirements of AAS. The module level test results thus far look very promising. However, the integration, performance test, and high-accuracy calibration for AAS will face many technical challenges.

Acknowledgments: The authors wish to thank Gerard van den Eijkel (DEMCON), Eddy van Brug (TNO), and Jing Zou (TNO) for reviewing the optical design and for valuable suggestions.

References

[1] O. Torres, P. K. Bhartia, J. R. Herman, Z. Ahmad and J. Gleason, J. Geophys. Res. 103, 17099–17110 (1998).
[2] J. R. Herman and P. K. Bhartia, J. Geophys. Res. 102, 16911–16922 (1997).
[3] J. P. Burrows and K. V. Chance, in ‘Optical Methods in Atmospheric Chemistry’. (SPIE, 1992).
[4] J. de Vries, G. H. J. van den Oord, E. Hilsenrath, M. B. J. te Plate, P. F. Levelt, et al., in ‘Proc. SPIE 4480’ (2002). DOI: 10.1117/12.453354.
[5] M. Dittman, E. Ramberg, M. Chrisp and J. V. Rodriguez, Proc. SPIE 4814, 111–119 (2002).
[6] J. P. Veefkind, I. Aben, K. McMullan, H. Försterd, J. de Vries, et al., Remote Sens. Environ. 120, 70–83 (2012).
[7] K. Yang, R. Dickerson, S. A. Carn, C. Ge, J. Wang. Geophys. Res. Lett. 40, 4957–4962 (2013).
[8] O. Torres, A. Tanskanen, B. Veihelmann, C. Ahn, R. Braak, et al., J. Geophys. Res. 112, D24S47 (2007). DOI: 10.1029/2007JD008809.
[9] Y. M. Wang, Y. J. Wang, W. H. Wang, Z. Mou, Z. J. G. Lü, et al., Chin. Sci. Bull. 55, 84–89 (2010).
[10] H. Visser and B. Snijders, US Patent 5841575 (1998).
[11] D. Nijkerk, B. van Venrooy, P. van Doorn, R. Henselmans, F. Draaisma, et al., in ‘ICSO’ (2012).
[12] J. Pan and P. Hao, Acta Astronom. Sin. 13, 46–56 (1965).
[13] Q. Liu, Z. Zhou, Y. Jin and W. Shen, in: ‘SPIE, Large Mirrors and Telescopes, vol. 9682L’ (2016).
[14] J. Caron, B. Sierk, J. L. Bezy, A. Loescher and Y. Meijer, in ‘ICSO’ (2014).
[15] Q. Xue, Acta Opt. Sin. 41, 0316003 (2014).
[16] M. Dobber, R. Voors, R. Dirksen, Q. Kleipool and P. Levelt, Solar Phys. 249, 281–291 (2008).

Entao Shi
Laboratory of Space Environment Exploration, National Space Science Center Chinese Academy of Sciences, Beijing 100190 China; School of Astronomy and Space Science, University of Chinese Academy of Sciences, Beijing 100049, China; Beijing Key Laboratory of Space Environment Exploration Beijing 100190, China; and Key Laboratory of Environmental Space Situation Awareness Technology, Beijing 100190, China
http://orcid.org/0000-0001-6821-3318

Entao Shi received a BS degree in applied physics in 2005 from Haerbin University of Science and Technology, China, and an MS degree in optical engineering in 2010 from Beijing Institute of Technology, China, and PhD degree in optical remote sensing from the Chinese Academy of Science, China, in 2018. He is an associate researcher in National Space Science Center, Chinese Academy of Science, since July 2010. Since then, he has been engaged in meteorological satellite payload instrument development including optical system design, mechanical design, alignment, etc. He is currently working on the AAS project on Gao-Fen 5B and Hyperspectral UV Total Ozone Unit (HTOU) on the FenYun-3F meteorological satellite.

Yongmei Wang
Laboratory of Space Environment Exploration, National Space Science Center, Chinese Academy of Sciences Beijing 100190, China; School of Astronomy and Space Science, University of Chinese Academy of Sciences, Beijing 100049, China Beijing Key Laboratory of Space Environment Exploration, Beijing 100190, China; and Key Laboratory of Environmental Space Situation Awareness Technology, Beijing 100190, China
Tel.: +86-10-62582751
wym@nssc.ac.cn

Yongmei Wang received a BS degree in atmosphere physics in 1989 from Chengdu University of Information Technology, China, and MS and PhD degrees in space physics from the Center for Space Science and Applied Research, Chinese Academy of Sciences, in 1996 and 2003, respectively. She is interested in optical remote sensing for atmosphere and space weather. Since 2001, she has worked in the field of development of optical instruments for atmospheric trace gas and aerosol measurement. She has been responsible for the Total Ozone Unit (TOU) onboard the FengYun-3B/C satellite of China. She is also the current Project Manager of AAS on Gao-Fen 5B and Hyperspectral UV Total Ozone Unit (HTOU) on the FenYun-3F meteorological satellite.

Nan Jia
Laboratory of Space Environment Exploration
National Space Science Center
Chinese Academy of Sciences
Beijing 100190, China

Nan Jia received his master's degree from University of Science and Technology Beijing in 2014. He is currently an engineer at the National Space Science Center of the Chinese Academy of Sciences (NSSC). He is working on research satellite photoelectric detection equipment.

Jinghua Mao
Laboratory of Space Environment Exploration
National Space Science Center
Chinese Academy of Sciences
Beijing 100190, China

Jinghua Mao received a PhD degree in space environment exploration from the Chinese Academy of Sciences, Beijing, China, in 2017. She is currently a research assistant with the National Space Science Center, Chinese Academy of Sciences. She is working on the calibration of satellite instruments.

Guanda Lu
Laboratory of Space Environment Exploration
National Space Science Center
Chinese Academy of Sciences
Beijing 100190, China

Guanda Lu received an MS degree in electrical engineering from Beijing Institute of Technology, Beijing, China, in 2018. His thesis was on reducing the current ripple of converters by using SiC Mosfet. He is currently a research assistant with the National Space Science Center, China Academy of Science, Beijing. He is working on the electrical design of Gao-Fen 05B satellite instruments.

Shaolin Liang
Laboratory of Space Environment Exploration, National Space Science Center Chinese Academy of Sciences, Beijing 100190 China; School of Astronomy and Space Science, University of Chinese Academy of Sciences, Beijing 100049, China; Beijing Key Laboratory of Space Environment Exploration Beijing 100190, China; and Key Laboratory of Environmental Space Situation Awareness Technology, Beijing 100190, China

Shaolin Liang received a BS degree in electronic science and technology from North China Electric Power University, Beijing, China, in 2014, and is currently a doctoral candidate at the University of Chinese Academy of Sciences. He is currently working on the CCD imaging system of the FY-3 project. His interests include the design, realization, test, and correction of the MCP/CCD/CMOS detector.